



## *In silico* and pharmacological study of *N,S*-acetal juglone derivatives as inhibitors of the P2X7 receptor-promoted *in vitro* and *in vivo* inflammatory response

Paulo Anastácio Furtado Pacheco<sup>a</sup>, Juliana Vieira Faria<sup>b,c</sup>, Ana Cláudia Silva<sup>b</sup>,  
Natalia Lidmar von Ranke<sup>d</sup>, Robson Coutinho Silva<sup>e</sup>, Carlos Rangel Rodrigues<sup>d</sup>,  
David Rodrigues da Rocha<sup>a</sup>, Robson Xavier Faria<sup>b,c,\*</sup>

<sup>a</sup> Department of Organic Chemistry, Institute of Chemistry, Fluminense Federal University, Campus do Valonguinho, Niterói, Rio de Janeiro, Brazil

<sup>b</sup> Laboratory for Evaluation and Promotion of Evaluation and Promotion of Environmental Health, Oswaldo Cruz Institute, Oswaldo Cruz Foundation, Rio de Janeiro, Brazil

<sup>c</sup> Postgraduate Program in Sciences and Biotechnology, Biology Institute, Universidade Federal Fluminense, Niterói, Rio de Janeiro, Brazil

<sup>d</sup> Laboratory of Molecular Modeling and QSAR (ModMolQSAR), Faculty of Pharmacy, Federal University of Rio de Janeiro, Rio de Janeiro, Brazil

<sup>e</sup> Laboratory of Immunophysiology, Biophysics Institute Carlos Chagas Filho, Federal University of Rio de Janeiro, Rio de Janeiro, Brazil

### ARTICLE INFO

#### Keywords:

Purinergic receptors  
P2X7R  
ATP  
Inflammation  
Drug  
Naphthoquinone

### ABSTRACT

Purinergic receptors are transmembrane proteins responsive to extracellular nucleotides and are expressed by several cell types throughout the human body. Among all identified subtypes, the P2×7 receptor has emerged as a relevant target for the treatment of inflammatory disease. Several clinical trials have been conducted to evaluate the effectiveness of P2×7R antagonists. However, to date, no selective antagonist has reached clinical use. In this work, we report the pharmacological evaluation of eleven *N, S*-acetal juglone derivatives as P2×7R inhibitors. Using *in vitro* assays and *in vivo* experimental models, we identified one derivative with promising inhibitory activity and low toxicity. Our *in silico* studies indicate that the 1,4-naphthoquinone moiety might be a valuable molecular scaffold for the development of novel P2×7R antagonists, as suggested by our previous studies.

### 1. Introduction

Purinergic signaling is involved in several physiological and pathological processes, such as immune responses, inflammation, pain, platelet aggregation, exocrine and endocrine secretion, endothelium-mediated vasodilation, cell proliferation, and death [1]. This system is composed of three essential elements: (1) extracellular purine or pyrimidine ligands, (2) transmembrane glycoproteins (purinergic receptors), and (3) ectonucleotidases, which regulate the concentration of extracellular nucleotides [2]. Based on pharmacological, biochemical, and molecular studies, these receptors are classically categorized as adenosine-activated receptors (P1 receptors) and nucleotide-responsive receptors (P2 receptors) [3,4].

P2 receptors are further structurally and functionally subdivided into two subfamilies: P2YRs, which are metabotropic receptors activated by

ATP and other nucleotides such as ADP, UTP, UDP, and UDP-glucose, and P2XRs, which are ATP-gated ion channels [5]. To date, seven P2XRs have been identified in mammal tissues (P2×1R-P2×7R) [6]. Our research group has focused on the development of P2×7R antagonists since this subtype has been directly involved in several inflammatory diseases and neuropathic pain [7,8]. This receptor can be distinguished from other P2XR subtypes because of its longer intracellular carboxy-terminal and reduced ATP sensitivity, demanding higher concentrations for activation ( $EC_{50} \geq 100 \mu\text{M}$ ) [9]. In addition, stimulation in the millimolar range (mM) and for a prolonged time induces an increase in membrane permeability by forming a nonselective pore, that allows the passage of molecules with 900 Da [10,11]. Depending on the cell type, several signaling pathways are also activated upon P2×7R stimulation, such as activation of the NLRP3 inflammasome and release of pro-inflammatory IL-1  $\beta$  [12]; stress-activated kinases pathway,

\* Corresponding author at: Laboratory for Evaluation and Promotion of Evaluation and Promotion of Environmental Health, Oswaldo Cruz Institute, Oswaldo Cruz Foundation, Rio de Janeiro, Brazil.

E-mail address: [salvador@ioc.fiocruz.br](mailto:salvador@ioc.fiocruz.br) (R.X. Faria).

<https://doi.org/10.1016/j.bioph.2023.114608>

Received 17 February 2023; Received in revised form 23 March 2023; Accepted 24 March 2023

Available online 30 March 2023

0753-3322/© 2023 The Authors. Published by Elsevier Masson SAS. This is an open access article under the CC BY license (<http://creativecommons.org/licenses/by/4.0/>).

leading to apoptosis [13]; mitogen-activated kinases (MAPK) pathway, leading to the production of reactive oxygen species and nitrogen intermediates [14]; and activation of phospholipase D with stimulation of lysosome-phagosome fusion [15]. In recent years, we have reported several molecular scaffolds of P2X<sub>7</sub> receptor inhibitors, such as triazole analogs, naphthoquinone derivatives, aryl boronic acids, and natural product-derived substances [16–21]. Recently, we have shown the potential antitrypanosomal activity of a group of juglone-derived *N*, *S*-acetal derivatives with low cytotoxicity [22]. Motivated by these promising results, and considering that the development of Chagas disease involves a high inflammatory response in both the acute and chronic phases [23], we decided to perform an initial screening of these compounds in P2X<sub>7</sub>-mediated inflammatory models. Herein, we report the identification of a potential 1,4-naphthoquinone-based inhibitor of *in vitro* and *in vivo* P2X<sub>7</sub>-mediated inflammatory responses.

## 2. Material and methods

### 2.1. *In vitro* and *in vivo* experiments

#### 2.1.1. Animals

All experiments followed Brazilian and institutional regulations and guidelines concerning animal experimentation. Animals were obtained from the animal breeding unit at the Oswaldo Cruz Foundation (FIOCRUZ, Rio de Janeiro, Brazil). P2X<sub>7</sub>-knockout mice were donated by the Immunophysiology laboratory of the Carlos Chagas Filho Biophysics Institute of the Federal University of Rio de Janeiro (IBCCF-UFRJ). Swiss Webster mice were maintained with PURINE-LABINE balanced ration, water "*ad libitum*" and a light–dark cycle of 12 h, before experimentation. All experimental procedures performed on mice were approved by institutional Committees of Animal Research Ethics in Oswaldo Cruz Foundation (CEUA-IOC, license number L039/2016) and in the Federal University of Rio de Janeiro (CEUA-UFRJ, license number 114/5).

#### 2.1.2. Isolation of murine peritoneal macrophages

Peritoneal macrophages were harvested from male Swiss Webster (weighing 20–30 g) through peritoneal lavage. The abdomen was sterilized, and a small incision was made to retract the abdominal skin and expose the peritoneum. Carefully, 10 mL of sterile phosphate buffered saline (PBS) was injected into the left side of the peritoneal wall of each mouse. Afterward, the peritoneum fluid was collected and centrifuged at 1500 rpm for 5 min. The supernatant was discarded, and the pellet was resuspended in 1 mL of cold RPMI for cell counting.

#### 2.1.3. Resazurin reduction assay

Peritoneal macrophages were plated into 96-well plates in complete RPMI 1640 medium (10% inactivated fetal bovine serum (FBS) + 1% antibiotic) for 24 h. For evaluation of the effect of the compound on mitochondrial metabolism, the medium was replaced by serum-free media, and treatments were performed with each NSA derivative diluted in DMSO at different concentrations (0.001–100 μM). After 72 h, 20 μL (0.15 mg/mL) of resazurin reagent (resazurin sodium salt, Sigma-Aldrich, St. Louis, MO, USA) were added to each well in the absence of light and the plates were further incubated for 3 h. Resazurin reduction was measured in a spectrophotometer (excitation wavelength = 570 nm and emission wavelength = 595 nm) using a SpectraMax M5 spectrophotometer (Molecular Devices, San Jose, CA, USA). Statistical data analysis was performed using GraphPad Prism 8 (GraphPad Software, Boston, MA, USA).

#### 2.1.4. LDH release assay

Peritoneal macrophages were cultured, as previously described, and treated with NSA derivatives for 72 h. Then, 50 μL/well was collected and transferred to another plate for LDH measurement using the CytoTox 96® Non-Radioactive Cytotoxicity Assay Kit (Promega, Madison, WI, USA). Absorbance was measured at 490 nm using a SpectraMax M5

spectrophotometer (Molecular Devices, San Jose, CA, USA).

#### 2.1.5. L929 cell culture for macrophage colony-stimulating factor (M-CSF) harvesting

L929 cells were donated by the Immunophysiology Laboratory of IBCCF-UFRJ and maintained according to their protocol. After thawing, cells were kept in complete RPMI medium until cell confluence. The supernatant containing macrophage colony-stimulating factor (M-CSF) was collected and reserved for further assays.

#### 2.1.6. Extraction and differentiation of macrophages extracted from P2X<sub>7</sub>-knockout bone marrow

Six P2X<sub>7</sub>-wild-type mice and six P2X<sub>7</sub>-knockout (P2X<sub>7</sub>-KO) mice (weighing 20–30 g), were donated by the laboratory of Immunophysiology of the IBCCF-UFRJ. Bone marrow was harvested shortly after the animal's euthanasia. After the extraction of the femur and tibia bones, a fissure was opened at one extremity, allowing the removal of medullary content through centrifugation at 1500 rpm for 5 min. The pellet was resuspended in supplemented RPMI medium (20% FBS, 30% L929- M-CSF-enriched supernatant, and 1% antibiotic) for differentiation into M2-type macrophages. Cells were maintained in this medium for one week until full differentiation.

#### 2.1.7. Dye uptake assays

ATP-induced dye uptake assays were performed on harvested peritoneal macrophage cells, using propidium Iodide (PI) (Sigma-Aldrich, St. Louis, MO, USA). P2X<sub>7</sub>-wt and P2X<sub>7</sub>-KO peritoneal macrophage cells were plated at a density of 3 × 10<sup>5</sup> cells/well. Cells were pretreated for 10 min with increasing concentrations of NSA molecules (0.01–100 μM) or with Brilliant Blue G (BBG) (750 nM). The incubation was carried out in a water bath at 37 °C. Afterward, the cells were stimulated with ATP (5 mM) for 15 min. PI (1 μM) was added in the final 5 min of incubation. Triton X-100 was used as a positive control and added 5 min before PI. Plate fluorescence was acquired using a SpectraMax M5 spectrophotometer (wavelengths of 520–600 nm).

#### 2.1.8. ATP-induced IL-1β release assay

Peritoneal macrophages (5 × 10<sup>5</sup> cells/well), not primed with LPS, were treated with ATP (5 mM) for 30 min, in the presence or absence of BBG (750 nM) and NSA15 (10 μM). Then, the plate was centrifuged at 500x g for 5 min. Supernatant from each well was collected and frozen until reading. IL-1β release was measured following the manufacturer's instructions (Mouse IL-1β Flex Set, Becton, Dickinson and Company, NJ, USA) using a BD FACS Calibur Flow Cytometer (Becton, Dickinson and Company, NJ, USA).

#### 2.1.9. Hemolysis assay

Blood from healthy donors was collected in sodium citrate-containing tubes. Red blood cells were collected by centrifugation at 2200 rpm for 10 min, and then washed three times with PBS. After this process, a red blood cell suspension was incubated with NSA15 (10 μM) for 3 h in a water bath at 36.5 °C. Triton X-100 0.5% was used as the positive control. After centrifugation at 1200 rpm for 3 min, absorbance was measured using a FlexStation 3 microplate reader (Molecular Devices, San Jose, CA, USA) at a wavelength of 578 nm.

#### 2.1.10. Paw edema model by extracellular ATP

Animals were separated into 5 different groups: saline (negative control), ATP (10 mM/paw), BBG (2.5 mg/kg), NSA15 (0.01 mg/kg) and NSA15 (0.1 mg/kg). Before paw edema induction, saline, BBG, or NSA15 (0.01 mg/kg and 0.1 mg/kg) were administered intraperitoneally according to their corresponding group. After one hour, 50 μL of ATP (10 mM/paw) was injected via a subplantar to induce local inflammation Sixty minutes after induction, paw volume was measured using a plethysmometer (UGO BASILE, Gemonio, Italy).

### 2.1.11. Peritonitis assay

Animals (five animals per group, aged 3–4 weeks) were treated intraperitoneally with sterile saline, NSA15 (0.01 or 0.1 mg/kg), BBG (2.5 mg/kg), and/or carrageenan (10 mg/kg). After one hour, saline (100  $\mu$ L) or carrageenan (10 mg/kg) was administered by the same route. At the end of the experiment, animals were euthanized and 10 mL of 1X PBS containing 10 mM EDTA was injected into the peritoneal cavity. Peritoneal fluid was collected and divided into two different tubes: 6.0 mL for the total leukocyte count and 1.5 mL for the differential count. Then, the tubes were centrifuged at 3500 rpm for 5 min. For total leukocyte count, the pellet was resuspended in 1.0 mL of Turk's liquid and counted in a quadrant of a Neubauer chamber. In the differential count, a squash-type smear was made with the pellet and the slides were stained with Giemsa.

## 2.2. In silico experiments

### 2.2.1. Ligands and target preparation

The ligand structures were built by Spartan10 v.1.0.1 (Wavefunction Inc., Irvine, CA, USA, 2000). The local minimum energy conformers were obtained using the MMFF94 force field [24]. The selected conformer was submitted to equilibrium geometry by applying the RM1 (Recife Model 1) semiempirical method [25]. The three-dimensional structure of the human P2 $\times$ 7 ion channel model was built as described in Faria et al., 2018 [26].

### 2.2.2. Molecular docking

To identify the NSA15 binding mode on P2 $\times$ 7R, we performed blind molecular docking on the whole receptor structure. To validate and compare the results we performed a redocking with the ligand A804598,

a selective antagonist for P2 $\times$ 7R. The ligands were previously prepared using AutoDock tools 4.2.6 (CCSB, La Jolla, CA, USA), which included the addition of hydrogen atoms as well as Gasteiger charges. For the molecular docking assay, we used the AutoDock Vina program (CCSB, La Jolla, CA, USA).

### 2.2.3. Pharmacokinetics and toxicological profile

The prediction of the pharmacokinetics and toxicological profile were performed by ADMET Predictor® (Simulation Plus, Lancaster, CA, EUA).

## 3. Results

### 3.1. Cytotoxicity evaluation

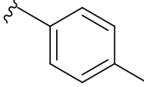
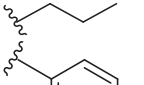
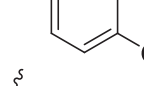
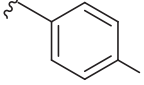
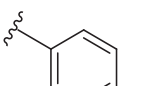
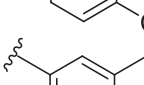
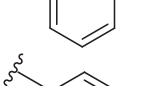
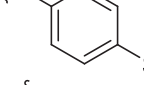
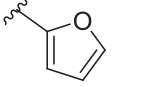
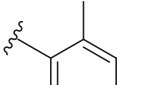
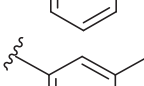
In this study, we evaluated the potential P2 $\times$ 7R antagonist activity of 11 juglone-derived *N,S*-acetal analogs that were synthesized as previously reported (Table 1) [22].

To assess the cytotoxic potential of all naphthoquinone derivatives, we performed the resazurin reduction assay, which evaluates the reductive metabolism of mammalian cells through the conversion of the resazurin dye (blue color) into resorufin dye (pink color and highly fluorescent). Initially, we evaluated the effect of increasing concentrations (0.001  $\mu$ M, 0.01  $\mu$ M, 0.1  $\mu$ M, 1  $\mu$ M, 10  $\mu$ M and 100  $\mu$ M) on mitochondrial metabolism. One derivative, NSA15, with a long aliphatic chain, showed the lowest toxicity toward peritoneal macrophages compared to other molecules. Table 2 presents the CC<sub>50</sub> for all compounds (Table 2). This cytotoxic profile of the NSA series was confirmed through LDH release assay, except for NSA2 and NSA15 (Table 2), as previously published [22].

**Table 1**  
Chemical structures of NSA compounds.

Reference	Chemical Structure	Reference	Chemical Structure
NSA1		NSA8	
NSA2		NSA9	
NSA4		NSA11	
NSA5		NSA14	
NSA6		NSA15	
NSA7			

**Table 2**  
CC<sub>50</sub> (μM) values for NSA compounds.

Compounds	R <sup>a</sup>	CC <sub>50</sub> (μM) <sup>1</sup>	CC <sub>50</sub> (μM) <sup>b</sup>
NSA1		0.7165	0.3684
NSA2		4.11	1.567
NSA4		0.2664	0.2598
NSA5		0.2104	0.3174
NSA6		0.762	0.1924
NSA7		7.642	1.187
NSA8		1.582	0.2258
NSA9		1.886	0.2343
NSA11		0.9858	0.264
NSA14		1.402	0.2231
NSA15		80.94	28.04

<sup>a</sup> resazurin assay.

<sup>b</sup> LDH assay.

### 3.2. In vitro evaluation of the P2×7R inhibitory activity of NSA compounds

As the induction of a nonselective pore is a hallmark of P2×7 receptor activation, we evaluated the activity of the NSA series, using the dye uptake assay. Initially, peritoneal macrophages were preincubated with NSA molecules (10 μM) for 10 min. Then, the cells were stimulated with ATP (5 mM) for more than 15 min and propidium iodide (PI) was added in the last 5 min. As shown in Fig. 1, only three molecules exhibited a significant inhibitory profile (NSA02, NSA05, and NSA15). Considering the better toxicity profile, we selected only the derivative NSA15 for further studies.

For IC<sub>50</sub> value determination, cells were incubated with increasing concentrations (0.01 nM – 100 μM) of NSA15 for 15 min before ATP stimulation. This compound exhibited a partial antagonist inhibitory profile with an IC<sub>50</sub> value of 963 nM (Fig. 2).

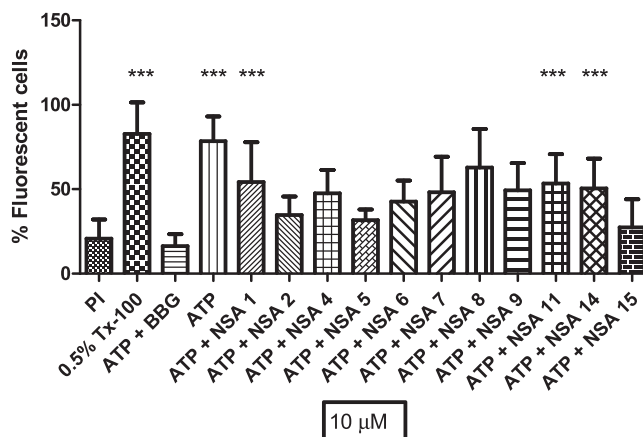


**Fig. 1.** Inhibition of ATP-induced dye uptake in the presence of the NSA series in peritoneal macrophages. Cells ( $3 \times 10^5$  cells/well) were treated with NSA compounds (10 μM) for 10 min. Then, ATP (5 mM) was added to each well for 15 min, and PI (5 μM) was added in the last 5 min. The experiments were performed in triplicate on at least three different days. ANOVA with post-hoc Tukey's test (\*\*\*)  $p < 0.0001$  compared with the PI bar.

We also performed dye uptake assays on bone marrow-derived P2×7R knockout macrophages. As observed in Fig. 4, cells treated with NSA15 exhibited the same uptake profile as the ATP control, suggesting that this compound might be in fact acting on P2×7R. It has been shown that ivermectin can potentiate the ATP action on the P2×4 receptor [27–29]. In fact, cotreatment with ivermectin induced higher ATP-mediated dye uptake, which was not reversed by NSA15 treatment. These results together corroborate the potential selective action of NSA15 on P2×7R (Fig. 3).

In addition, we also evaluated the effect of NSA15 on P2×7R-mediated IL-1β release in peritoneal macrophages (Fig. 4). Treatment with ATP (5 mM) alone induced the release of IL-1β in macrophages not primed with LPS, which was reversed by treatment with BBG. In contrast, treatment with NSA15 (10 μM) alone did not result in a significant increase in this cytokine. In agreement with the dye uptake assay, treatment with NSA15 inhibited the ATP-induced IL-1β release (Fig. 4).

### 3.3. In silico assays

#### 3.3.1. Molecular docking

The redocking results with A804598, the reference P2×7R antagonist, reproduced most of its interaction at the allosteric binding site, particularly the hydrophobic interactions that occur with Phe109, Phe88, Phe95, Met105 and Try295. The superposition of the crystalline structure of the A804598 ligand and the conformation generated by redocking are presented in Fig. 5.

The docking results of NSA15 against P2×7 indicated that the most populated cluster is in the same allosteric site of the ligand A804598, as characterized for other antagonists identified by Kawate & Karasawa [30]. In the allosteric site, two potential conformational poses have been identified for compound NSA15. For both conformations, the juglone (5-hydroxy-1,4-naphthalenedione) moiety is oriented in the same position as the quinolone moiety of A804598, which performs hydrophobic interactions with Phe88, Met105 and Phe108 (Fig. 6). Such interactions suggest that the juglone moiety is an important fragment that should be preserved in the molecule for interaction with the allosteric site. However, it was observed that in one possible conformation (Fig. 6A), the hydrophobic chain is oriented outside the ion channel groove and interacts with Val84. In the other conformation (Fig. 6B), the hydrophobic chain is oriented inward from the ion channel groove and interacts with Try295 and Phe95. Additionally, the NSA15 and the A804598 ligand present similar binding energy values (Table 3), indicating a potential

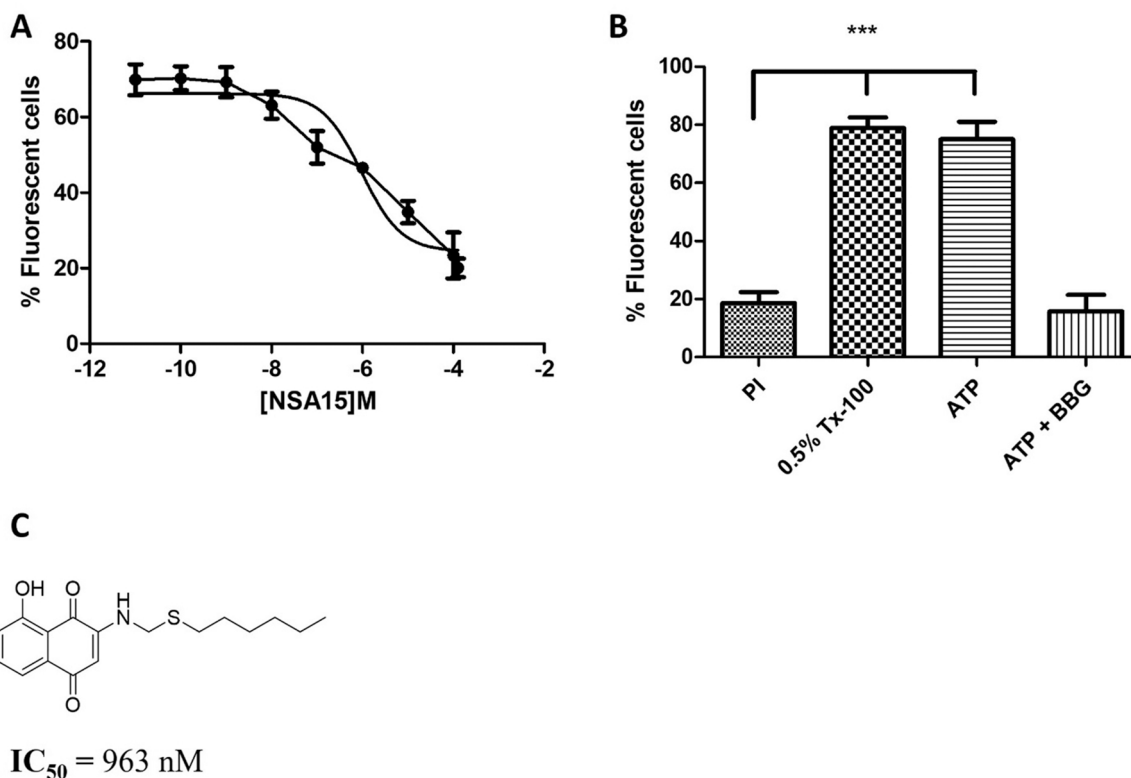


**Fig. 2.** Inhibition of ATP-induced dye uptake in the presence of NSA15 in peritoneal macrophages. Dose—response curve (A) and (B) experimental controls. Cells ( $3 \times 10^5$  cell/well) were treated with increasing concentrations of NSA15. After preincubation for 10 min, the cells were exposed to ATP (5 mM) for more than 15 min. In the last 5 min, PI (5  $\mu$ M) was added to each well. (C) NSA15 structure with  $IC_{50}$  values obtained from the dye uptake assay. The experiments were performed in triplicate on at least three different days. ANOVA with post-hoc Tukey’s test (\*\*\*)  $p < 0.0001$  compared with the PI bar.

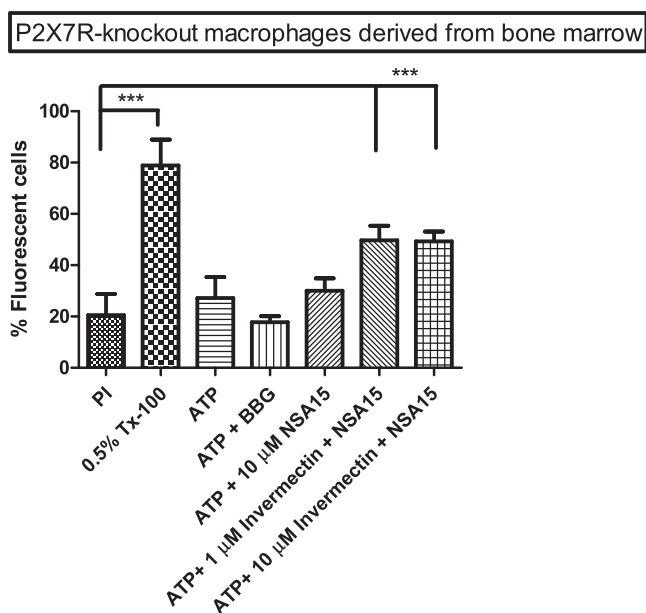


**Fig. 3.** Cell permeabilization assays in P2X7R-knockout macrophages. Cells ( $3 \times 10^5$  cells/well) were treated with NSA15 for 10 min. Then, the cells were treated with ATP for more than 15 min. Ethidium bromide (BE) was added in the last 5 min. The experiments were performed in triplicate on at least three different days. ANOVA with post-hoc Tukey’s test (\*\*\*)  $p < 0.05$  compared with the PI bar.

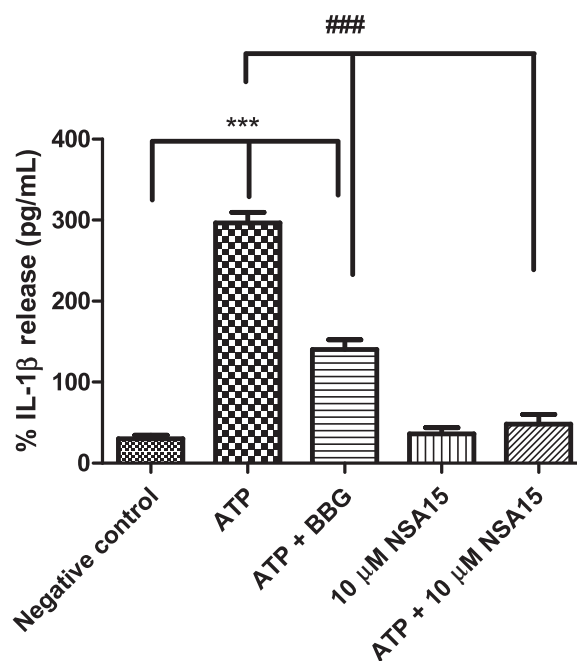


**Fig. 4.** Inhibition of ATP-induced IL-1 $\beta$  release by NSA15 in peritoneal macrophages. Cells ( $5 \times 10^5$  cells/well) were treated with ATP (5 mM) for 30 min in the presence or absence of NSA15 (10  $\mu$ M) and BBG (750 nM). The plate was centrifuged (500x g for 5 min), and its supernatant was removed and analyzed by flow cytometry (BD FACS Calibur). ANOVA with post-hoc Tukey’s test (\*\*\*)  $p < 0.01$  compared to the PI bar; (###)  $p < 0.05$  compared to treatment with ATP.



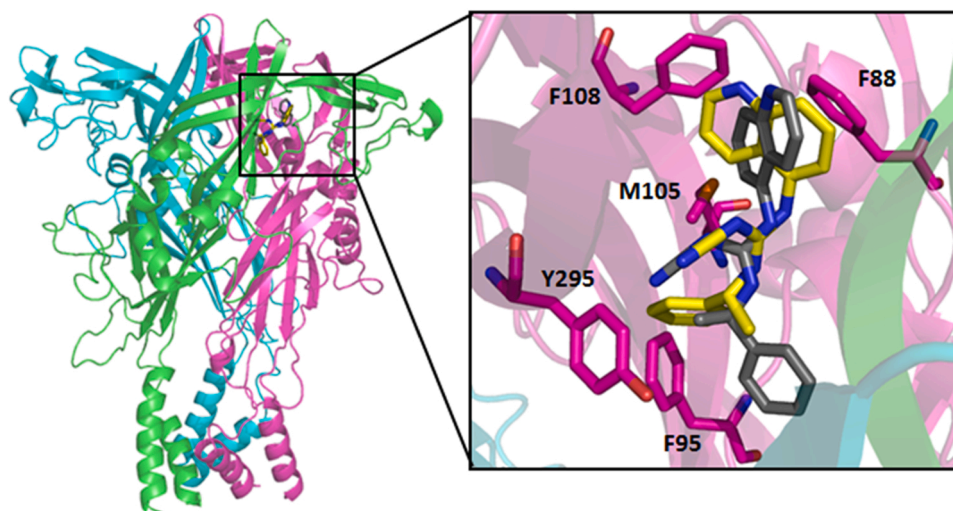


**Fig. 5.** Representation of the redocking result of ligand A804598 against P2 $\times$ 7R. The receptor is represented in cartoon form, and each chain is presented in a different color (pink, cyan and green). The A804598 conformation derived from the crystal P2 $\times$ 7R structure (PDB: 5U1V) is represented in yellow, and the A804598 conformation derived from refitting is represented in gray.

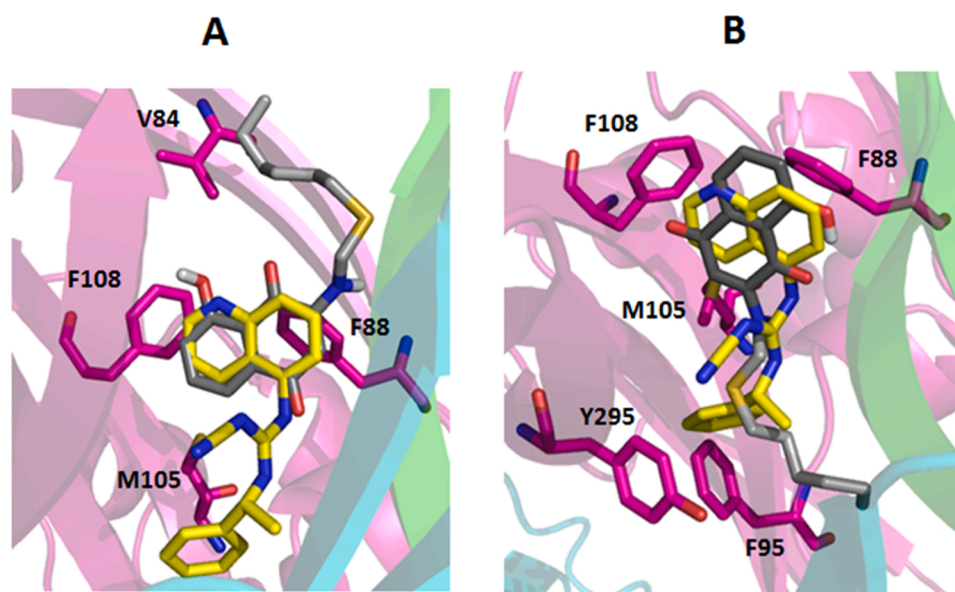


**Fig. 6.** Representation of the two most likely conformations of compound NSA15 (represented in gray) docked into P2 $\times$ 7R. (A) The hydrophobic chain is oriented outward the ion channel pore. (B) The hydrophobic chain is oriented inward from the channel pore. For comparison, this figure represents the superposition of the crystallographic structure of A804598 (represented in yellow).

**Table 3**

Binding energy (kcal/mol) of the two most favorable conformations of NSA15 (confirmation A and B) and the ligand A804598 into the P2 $\times$ 7 receptor.

Ligand	Binding energy (kcal/mol)
NSA15 (A)	-7.6
NSA15 (B)	-7.5
A804598	-8.1

affinity of NSA15 for the P2 $\times$ 7R.

### 3.3.2. *In silico* toxicity evaluation

The pharmacokinetic and toxicological properties of NSA15 were computationally predicted and compared to three widely used anti-inflammatory drugs (diclofenac, ibuprofen, and naproxen). As

**Table 4**

Physicochemical parameters of NSA15 and other approved anti-inflammatory drugs (diclofenac, ibuprofen, and naproxen).

Compounds	Physical-chemical Properties					
	MW <sup>a</sup>	LogP <sup>b</sup>	S+WS <sup>c</sup>	HBA <sup>d</sup>	HBD <sup>e</sup>	NLRB <sup>f</sup>
NSA15	319	2.54	0.027	4	2	0
Diclofenac	295	3.89	0.0464	3	2	0
Ibuprofen	206	3.0	0.1	2	1	0
Naproxen	230	2.69	0.0649	3	1	0

<sup>a</sup> Molecular weight (Da).

<sup>b</sup> Partition coefficient in a logarithmic scale.

<sup>c</sup> Native water solubility (mg/mL).

<sup>d</sup> Number of hydrogen bond acceptors (HBA).

<sup>e</sup> Number of hydrogen bond donors (HBD).

<sup>f</sup> Number of Lipinski's rules broken (NLRB).

indicated in Table 4, NSA15 exhibited physicochemical properties compatible with most approved oral drugs, as all analyzed parameters complied with Lipinski's rule.

Compared to the reference anti-inflammatory drugs (diclofenac, ibuprofen, and naproxen), NSA15 presented a different pharmacokinetic profile with low probability of crossing the blood-brain barrier, a lower jejunal permeability, a higher volume distribution, and a high potential of being a P-gp substrate (Table 5). Despite all those characteristics, the ADMET risk for NSA15 was inferior to that for diclofenac, for example.

As shown in Table 6, NSA15 presented a toxicological risk inferior to that of the reference drug diclofenac, with a low probability of inhibiting the human potassium channel (hERG), and low hepatotoxicity and reproductive toxicity. However, NSA15 presented a higher risk of mutagenicity.

### 3.4. Hemocompatibility Test

As a preliminary assessment of the potential toxic effect of NSA15 *in vivo*, we also conducted a hemocompatibility assay. Human red blood cells were incubated with NSA15 (10  $\mu$ M) for 3 h. A saline isotonic solution was used as a negative control. As observed in Fig. 7, treatment with NSA15 showed a negligible hemolytic effect (lower than 10% hemolysis) compared to the positive control.

### 3.5. *In vivo* anti-inflammatory evaluation

#### 3.5.1. Paw edema assay

To confirm the safety profile of NSA15 indicated by our *in vitro* assays, we performed an *in vivo* evaluation of acute toxicity. Swiss Webster mice were intraperitoneally treated with 10 mg/kg NSA15 for 24 h, and mortality and behavioral parameters were closely monitored. After this period, no animal showed signs of toxicity (data not shown). An ATP-induced paw edema assay was used to assess whether NSA15 could also exhibit *in vivo* anti-inflammatory activity. The animals were divided into five groups: saline (negative control), BBG (2.5 mg/kg), ATP (10 mM/paw), NSA15 (0.1 mg/kg) and NSA15 (0.01 mg/kg). A significant decrease in ATP-induced paw swelling was identified at the tested doses, suggesting that NSA15 exhibits anti-inflammatory action by reducing paw edema (Fig. 8). As observed for the BBG-treated group, the results indicated a significant decrease in ATP-induced paw edema in both groups treated with NSA15, corroborating our *in vitro* data.

#### 3.5.2. Carrageenan-induced peritonitis assay

We also studied the anti-inflammatory effect on carrageenan-induced cell migration to the peritoneal cavity. The animals were separated into five distinct treatment groups: saline (negative control), NSA15 (0.01 mg/kg), NSA (0.1 mg/kg), and BBG (2.5 mg/kg). After one hour, peritonitis was induced by intraperitoneal administration of

**Table 5**

Pharmacokinetics parameters of NSA15 and reference anti-inflammatory drugs (diclofenac, ibuprofen, and naproxen).

Compounds	Pharmacokinetics Parameters					
	BBB <sup>a</sup>	Peff <sup>b</sup>	RBP <sup>c</sup>	Vd <sup>d</sup>	P-gp <sup>e</sup>	ADMET_Risk <sup>f</sup>
NSA15	Low	3.937	0.694	0.67	Yes	2.35
Diclofenac	High	6.40	0.62	0.26	No	4
Ibuprofen	High	6.52	0.58	0.34	No	1.7
Naproxen	High	6.44	0.58	0.23	No	1.74

<sup>a</sup> Qualitative probability (High/Low) of crossing the blood-brain barrier (BBB).

<sup>b</sup> Human jejunal effective permeability ( $\text{cm/s} \times 10^4$ )(Peff).

<sup>c</sup> Blood-to-plasma concentration ratio in humans (RBP).

<sup>d</sup> Pharmacokinetic volume of distribution in humans (L/kg) (Vd).

<sup>e</sup> Probability of P-glycoprotein efflux (P-gp)

<sup>f</sup> ADMET\_Risk (probability of a compound being successfully developed as an orally bioavailable drug).

carrageenan (10 mg/kg). Three hours after the administration of carrageenan, peritoneal fluid was collected, and the total leukocyte count and differential count were determined. As expected, treatment with carrageenan led to an increase in the number of total leukocytes compared to the saline group (Fig. 9a). Pretreatment with the P2 $\times$ 7R antagonist BBG (2.5 mg/kg) inhibited leukocyte migration to the peritoneal cavity. Moreover, in both NSA15 treatment groups (0.01 mg/kg and 0.1 mg/kg), a decrease in the number of peritoneal leukocytes was observed (Fig. 9b and c), suggesting that this molecule may exert its anti-inflammatory action through P2 $\times$ 7R inhibition.

## 4. Discussion

The P2 $\times$ 7 receptor has been recognized as a relevant target for several human diseases, and there has been increasing interest in the development of selective antagonists [31–34]. In drug discovery, natural products and derivatives have historically been a valuable source of bioactive compounds or inspiration for the synthesis of novel pharmacological entities. In recent years, our group has identified and reported various naphthoquinone derivatives with anti-inflammatory activity through P2 $\times$ 7R inhibition [17,19,35–37]. Herein, we report *in vitro* and *in vivo* studies of eleven *N*, *S*-acetal juglone derivatives as P2 $\times$ 7 receptor inhibitors. Previously, we identified that two members of these compounds exhibited promising inhibitory activity against epimastigote and amastigote forms of *Trypanosoma cruzi* with low toxicity. Considering the high inflammatory response in both the acute and chronic phases of Chagas disease, we also decided to assess the potential anti-inflammatory activity of this family of compounds. Surprisingly, we identified that one of these compounds also exerted anti-inflammatory effects through inhibition of P2 $\times$ 7R. The compound NSA15, with a long aliphatic side chain, inhibited ATP-induced dye uptake and IL-1 $\beta$  release in peritoneal macrophages without significant toxicity. As observed in our previous studies [19], molecular docking at the allosteric site located in P2 $\times$ 7R suggests that the juglone motif is essential for the main molecular interactions, while the aliphatic side chain might be a position for further chemical modifications, aiming to increase affinity or pharmacokinetic properties. Together, these results agree with other studies that have shown an anti-inflammatory potential of juglone [38]. In fact, this naphthoquinone has been investigated for its antioxidant properties, which can be related to anti-inflammatory activity, since the production of reactive oxygen species and nitric oxide are well-known inducers of inflammation [39,40]. It has been shown that treatment with juglone alone inhibited and decreased the expression of the NLRP3 inflammasome and caspase-1 and, consequently, the release of IL-1 $\beta$  and IL-18 cytokines in the LPS-primed macrophage J774.1 [41]. Although in the present study, we did not evaluate the relationship with NLRP3 inflammasome activation directly, our *in vitro* and *in silico* studies support that this might also be a mechanism of action of the NSA15 derivative. We highlight that our results reinforce the juglone moiety as a valuable molecular platform for the synthesis of anti-inflammatory compounds targeting the P2 $\times$ 7R-NLRP3 inflammasome pathway, in agreement with our previous results and recent studies in the literature [19,38,42,43].

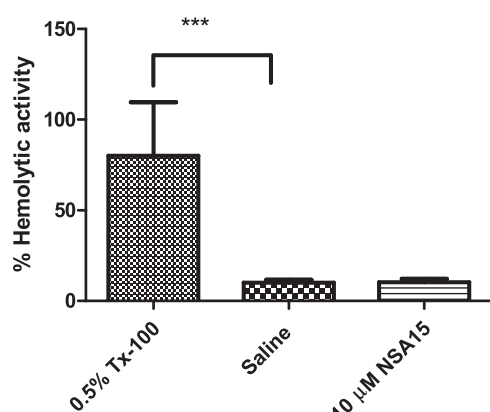
Additionally, we performed a dye uptake assay with P2 $\times$ 7R-knockout (KO) cells to evaluate whether these results are associated with selective receptor inhibition. Treatment of P2 $\times$ 7R-KO cells with NSA15 resulted in an uptake profile similar to that of the ATP control group. To exclude an influence of the P2 $\times$ 4 receptor on these results, we repeated the experiment assessing how NSA15 could influence the effect of ivermectin-on ATP-mediated P2 $\times$ 7R activation [27]. As expected, we observed that treatment with ivermectin potentiated the effect of ATP, resulting in an increase in dye uptake. Pretreatment with NSA15 did not change this effect, suggesting a selective action toward P2 $\times$ 7R.

Although NSA15 inhibition was observed using an ATP-induced dye uptake assay in mouse peritoneal macrophages, the association of the absence of an inhibitory effect of NSA15 on P2 $\times$ 7R-knockout (KO) cells,

**Table 6**

Toxicological profile of NSA15 and commercially available anti-inflammatory drugs (diclofenac, ibuprofen and naproxen).

Compound	hERG <sup>a</sup>	CABR <sup>b</sup>	Hepatotoxicity <sup>c</sup>			Repro <sup>d</sup>	MUT_Risk <sup>e</sup>	TOX_Risk <sup>f</sup>
			AlkPhos	GGT	LDH			
NSA15	No	Toxic	Normal	Normal	Normal	Nontoxic	1.8	1
Diclofenac	Yes	Nontoxic	Elevated	Elevated	Normal	Nontoxic	0.6	2
Ibuprofen	No	Nontoxic	Normal	Normal	Normal	Nontoxic	0.6	0
Naproxen	No	Toxic	Normal	Normal	Normal	Nontoxic	1.2	0

<sup>a</sup> Qualitative estimation of the probability of human potassium channel inhibition (hERG).<sup>b</sup> Qualitative estimation of triggering mutagenic chromosomal aberrations (CABR).<sup>c</sup> human liver adverse effect estimated as the probability of increasing plasma concentration of one of the following enzymes: Alkaline Phosphatase (AlkPhos), GGT, and LDH.<sup>d</sup> Qualitative estimation of reproductive toxicity.<sup>e</sup> Risk of mutagenicity assessed by ten models of “virtual Ames testing” (MUT\_Risk).<sup>f</sup> Overall toxicological risk (TOX\_Risk).

**Fig. 7.** Hemolytic assay. Human red blood cells were treated with NSA15 (10 μM). After 3 h, the supernatant was removed and placed in a 96-well plate for absorbance reading. The assay was performed in triplicate. ANOVA with post-hoc Tukey's test (\*\*\*) $p < 0.0001$  compared to the PI bar.

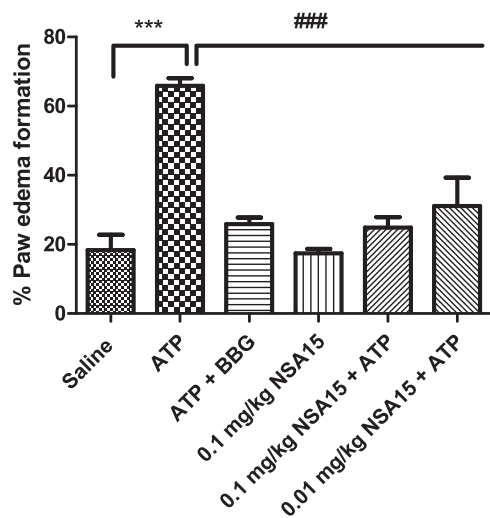


**Fig. 8.** ATP-induced paw edema assay results. Paw edema was induced by administration of ATP (10 mM/paw). Saline solution and BBG (2.5 mg/kg) were used as negative and positive controls, respectively. NSA15 (0.1 mg/kg and 0.01 mg/kg) was administered intraperitoneally one hour before the induction of inflammation in the paw. After 60 min, the paw volume was measured, and statistical analysis was performed. The experiments were carried out on at least three different days. ANOVA with post-hoc Tukey's test;  $p < 0.05$ , (\*\*\*) $p < 0.001$  compared with the PI bar. ### compared with ATP treatment.

and mouse peritoneal macrophages expressing wild-type P2×7R treated with ATP + ivermectin reinforces the NSA15 selectivity for P2×7R. NSA15 produced an effect with an inhibition value higher than that of BBG and similar to that of A740003. Additionally, *in silico* data exhibited NSA15 interaction with moieties on the allosteric P2×7R site, as observed for another selective P2×7R antagonist [30]. Therefore, these factors reinforce the selective NSA15 inhibition of P2×7R.

Since NSA15 demonstrated an adequate safety profile through different *in vitro* assays and *in vivo* through an acute toxicity experimental model, we evaluated P2×7R inhibition and anti-inflammatory activity *in vivo*, using ATP-induced paw edema and carrageenan-triggered peritonitis assays. We observed that pretreatment with NSA15 (0.01 mg/kg and 0.1 mg/kg) prevented the P2×7R-mediated inflammatory responses, comparable to the reference antagonist, BBG (2.5 mg/kg).

Inflammatory disorders are currently treated using glucocorticoids or nonsteroidal anti-inflammatory drugs (NSAIDs). While the first class of drugs acts through suppression of proinflammatory genes, NSAIDs act by direct inhibition of COX enzymes and prostaglandin biosynthesis. However, the chronic use of these drugs is commonly associated with undesired side effects. In this scenario, P2×7R has appeared as an alternative therapeutic target for the treatment of diseases with a chronic inflammatory background. Clinical trials have been conducted with P2×7R antagonists for the treatment of diseases such as rheumatoid arthritis (NCT00628095)[44], neurodegenerative diseases (NCT03918616)[45], and pain (NCT00849134) [46]. One example is the current clinical trial for depression therapy using the P2×7R antagonist JNJ-54175446, developed by Janssen Pharmaceuticals (NCT04116606)[47]. Following our previous works that have identified some putative P2×7R antagonist naphthoquinone-derived compounds, we tested a group of *N,S*-acetal juglone derivatives and report a set of *in vitro* and *in vivo* results that support the relevance of this molecular scaffold for the development of novel and selective inhibitors.

## 5. Conclusion

In this work, we tested eleven *N,S*-acetal juglone-derived compounds and identified one derivative (NSA15) capable of inhibiting *in vitro* (dye uptake and IL-1β release) and *in vivo* (ATP-induced paw edema and peritonitis) responses mediated by P2×7R activation, with a safe profile toward peritoneal macrophage cells. Our *in-silico* studies support that the 1,4-naphthoquinone moiety might be a valuable scaffold for the generation of novel and potent P2×7R antagonists.

## Ethical approval

All procedures performed in studies involving animals followed the institution's ethical standards or practice at which the studies were conducted.



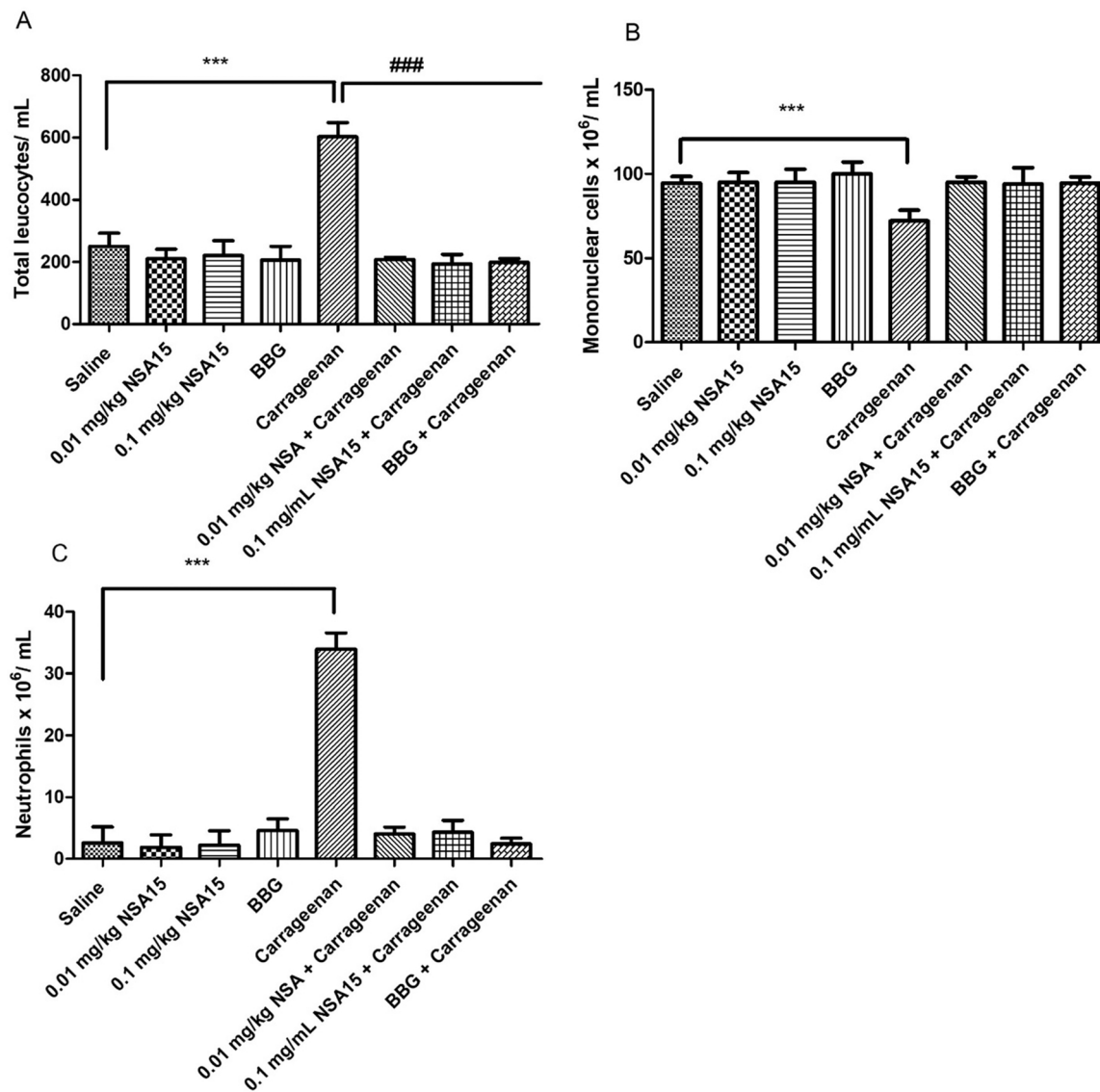


**Fig. 9.** Results of the carrageenan-induced peritonitis assay. Total leukocyte count (A) and differential count (B - C). Swiss webster mice were treated with saline, BBG (2.5 mg/kg), or NSA15 (0.01 mg/kg and 0.1 mg/kg) one hour before carrageenan administration (except saline) to induce inflammation. After three hours, the peritoneal liquid was collected and analyzed. These results are expressed as the mean  $\pm$  s.d. of three experiments on different days. \* \*\*p < 0.0001 compared to the saline or carrageenan group.

## Funding

The fellowships granted by CNPq (316568/2021-0), CAPES (Financial Code 001) and FAPERJ (E-26/203.246/2017, E-26/203.146/2017, E-26/211.025/2019, E-26/200.982/2021, and E-26/201.369/2021) are gratefully acknowledged.

## CRediT authorship contribution statement

J.V.F, A.C.S, and R.X.F - these authors did the biological assays. N.L.R. and C.R.R. - these authors did the in-silico assays. D.R.R. and P.A.F.P. - these authors planned and coordinated the synthesis of molecules. J.V.F., P.A.F.P., and R.X.F. - these authors - prepare the figures, wrote, and revised the paper. P.A.F.P., and R.X.F. - these authors revised the biological assays, wrote, and revised the paper.

## Conflict of interest statement

The authors declare that they have no conflict of interest.

## Data Availability

Data will be made available on request.

## Acknowledgments

We thank the IOC, LAPSA and PPGQ-UFF for their support.

## References

- [1] G. Burnstock, The therapeutic potential of purinergic signalling, *Biochem Pharm.* 151 (2018) 157–165, <https://doi.org/10.1016/j.bcp.2017.07.016>.
- [2] G.G. Yegutkin, Nucleotide- and nucleoside-converting ectoenzymes: important modulators of purinergic signalling cascade, *Biochim. Biophys. Acta Mol. Cell Res.* 1783 (2008) 673–694, <https://doi.org/10.1016/j.bbamcr.2008.01.024>.
- [3] V. Ralevic, G. Burnstock, Receptors for purines and pyrimidines, *Pharm. Rev.* 50 (1998) 413–492, [https://doi.org/10.1007/978-3-642-28863-0\\_5](https://doi.org/10.1007/978-3-642-28863-0_5).
- [4] G. Burnstock, Purinergic signalling: from discovery to current developments, *Exp. Physiol.* 99 (2014) 16–34, <https://doi.org/10.1113/expphysiol.2013.071951>.
- [5] K.A. Jacobson, J. Linden, *Pharmacology of purine and pyrimidine receptors*. Preface., 2011.

- [6] R.A. North, P2X receptors, *Philos. Trans. R. Soc. Lond. B Biol. Sci.* 371 (2016) 20150427, <https://doi.org/10.1098/rstb.2015.0427>.
- [7] W.A. Carroll, D. Donnelly-Roberts, M.F. Jarvis, Selective P2×7 receptor antagonists for chronic inflammation and pain, *Purinergic Signal* 5 (2009) 63–73, <https://doi.org/10.1007/s11302-008-9110-6>.
- [8] C.C. Chrovián, J.C. Rech, A. Bhattacharya, M.A. Letavic, P2×7 Antagonists as potential therapeutic agents for the treatment of CNS disorders, *Prog. Med Chem.* (2014) 65–100, <https://doi.org/10.1016/B978-0-444-63380-4.00002-0>.
- [9] N. Mehta, M. Kaur, M. Singh, S. Chand, B. Vyas, P. Silakari, M.S. Bahia, O. Silakari, Purinergic receptor P2×7: a novel target for anti-inflammatory therapy, *Bioorg. Med Chem.* 22 (2014) 54–88, <https://doi.org/10.1016/j.bmc.2013.10.054>.
- [10] R.X. Faria, F.P. DeFarias, L.A. Alves, Are second messengers crucial for opening the pore associated with P2×7 receptor? *Am. J. Physiol. Cell Physiol.* 288 (2005) C260–C271, <https://doi.org/10.1152/ajpcell.00215.2004>.
- [11] R.X. Faria, C.M. Cascabulho, R.A.M. Reis, L.A. Alves, Large-conductance channel formation mediated by P2×7 receptor activation is regulated through distinct intracellular signaling pathways in peritoneal macrophages and 2B4 cells, *Naunyn Schmiede Arch. Pharm.* 382 (2010) 73–87, <https://doi.org/10.1007/s00210-010-0523-8>.
- [12] P. Pelegrin, P2×7 receptor and the NLRP3 inflammasome: partners in crime, *Biochem Pharm.* 187 (2021), <https://doi.org/10.1016/j.bcp.2020.114385>.
- [13] B.D. Humphreys, J. Rice, S.B. Kertesz, G.R. Dubyak, Stress-activated protein kinase/JNK activation and apoptotic induction by the macrophage P2×7 nucleotide receptor, *J. Biol. Chem.* 275 (2000) 26792–26798, <https://doi.org/10.1074/jbc.M002770200>.
- [14] B. Wang, R. Slutyer, P2×7 receptor activation induces reactive oxygen species formation in erythroid cells, *Purinergic Signal* 9 (2013) 101–112, <https://doi.org/10.1007/s11302-012-9335-2>.
- [15] Y. Qu, G.R. Dubyak, P2×7 receptors regulate multiple types of membrane trafficking responses and non-classical secretion pathways, *Purinergic Signal* 5 (2009) 163–173, <https://doi.org/10.1007/s11302-009-9132-8>.
- [16] B.Q. Magalhães, F.P. Machado, P.S. Sanches, B. Lima, D.Q. Falcão, N.L. Von Ranke, M.L. Bello, C.R. Rodrigues, M.G. Santos, L. Rocha, R.X. Faria, Eugenia sulcata (Myrtaceae) nanoemulsion enhances the inhibitory activity of the essential oil on P2×7R and inflammatory response in vivo, *Pharmaceutics* 14 (2022) 911.
- [17] J.P.S. dos Santos, R.C.B. Ribeiro, J.V. Faria, M.L. Bello, C.G.S. Lima, F.P. Pauli, A. A. Borges, D.R. Rocha, M.G. Moraes, L.S.M. Forezi, V.F. Ferreira, R.X. Faria, F. de C. da Silva, Synthesis, biological evaluation and molecular modeling studies of novel 1,2,3-triazole-linked menadione-furan derivatives as P2×7 inhibitors, *J. Bioenerg. Biomembr.* (2022), <https://doi.org/10.1007/s10863-022-09947-2>.
- [18] D.T.G. Gonzaga, L.B.G. Ferreira, T.E. Moreira Maramaldo Costa, N.L. von Ranke, P. Anastácio Furtado Pacheco, A.P. Sposito Simões, J.C. Arruda, L.P. Dantas, H. R. de Freitas, R.A. de Melo Reis, C. Penido, M.L. Bello, H.C. Castro, C.R. Rodrigues, V.F. Ferreira, R.X. Faria, F. de, C. da Silva, 1-Aryl-1H- and 2-aryl-2H-1,2,3-triazole derivatives blockade P2×7 receptor in vitro and inflammatory response in vivo, *Eur. J. Med Chem.* 139 (2017) 698–717, <https://doi.org/10.1016/j.ejmech.2017.08.034>.
- [19] P.A.F. Pacheco, R.M.S. Galvão, A.F.M. Faria, N.L. Von Ranke, M.S. Rangel, T. M. Ribeiro, M.L. Bello, C.R. Rodrigues, V.F. Ferreira, D.R. da Rocha, R.X. Faria, 8-Hydroxy-2-(1H-1,2,3-triazol-1-yl)-1,4-naphthoquinone derivatives inhibited P2×7 receptor-induced dye uptake into murine macrophages, *Bioorg. Med. Chem.* 27 (2019) 1449–1455, <https://doi.org/10.1016/j.bmc.2018.11.036>.
- [20] J.C.C. Arruda, N.C. Rocha, E.G. Santos, L.G.B. Ferreira, M.L. Bello, C. Penido, T.E. M.M. Costa, J.A.A. Santos, I.M. Ribeiro, T.C.B. Tomassini, R.X. Faria, Physalin pool from *Physalis angulata* L. leaves and physalin D inhibit P2×7 receptor function in vitro and acute lung injury in vivo, *Bioomed. Pharmacother.* 142 (2021), <https://doi.org/10.1016/j.biopha.2021.112006>.
- [21] D.T. Gonzaga, F.H. Oliveira, J.P. Salles, M.L. Bello, C.R. Rodrigues, H.C. Castro, H. de Souza, C. Reis, R. Leme, J. Mafra, L. Pinheiro, L. Hoelz, N. Boechat, R. X. Faria, Synthesis, biological evaluation and molecular modeling studies of new thiadiazole derivatives as potent P2×7 receptor inhibitors, *Front Chem.* 7 (2019), <https://doi.org/10.3389/fchem.2019.00261>.
- [22] P.A.F. Pacheco, T. de Menezes Ribeiro, R.M. dos Santos Galvão, E.G. dos Santos, A. F.M. Faria, N.L. von Ranke, M.L. Bello, C.R. Rodrigues, V.F. Ferreira, A.L.A. Souza, D. de Jesús Haridoim, K. da Silva Calabrese, R.X. Faria, D.R. da Rocha, Synthesis of new N,S-acetal analogs derived from juglone with cytotoxic activity against *Trypanosoma cruzi*, *J. Bioenerg. Biomembr.* 52 (2020) 199–213, <https://doi.org/10.1007/s10863-020-09834-8>.
- [23] A. Talvani, M.M. Teixeira, Inflammation and chagas disease: some mechanisms and relevance, *Adv. Parasitol.* (2011) 171–194, <https://doi.org/10.1016/B978-0-12-385895-5.00008-6>.
- [24] T.A. Halgren, Merck molecular force field. I. Basis, form, scope, parameterization, and performance of MMFF94, *J. Comput. Chem.* 17 (1996) 490–519, [https://doi.org/10.1002/\(SICI\)1096-987X\(199604\)17:5<490::AID-JCC1>3.0.CO;2-P](https://doi.org/10.1002/(SICI)1096-987X(199604)17:5<490::AID-JCC1>3.0.CO;2-P).
- [25] G.B. Rocha, R.O. Freire, A.M. Simas, J.J.P. Stewart, RM1: A reparameterization of AM1 for H, C, N, O, P, S, F, Cl, Br, and I, *J. Comput. Chem.* 27 (2006), <https://doi.org/10.1002/jcc.20425>.
- [26] R.X. Faria, F.H. Oliveira, J.P. Salles, A.S. Oliveira, N.L. von Ranke, M.L. Bello, C. R. Rodrigues, H.C. Castro, A.R. Louvis, D.L. Martins, V.F. Ferreira, 1,4-naphthoquinones potentially inhibiting P2×7 receptor activity, *Eur. J. Med. Chem.* 143 (2018), <https://doi.org/10.1016/j.ejmech.2017.10.033>.
- [27] V. Latapiat, F.E. Rodríguez, F. Godoy, F.A. Montenegro, N.P. Barrera, J. P. Huidobro-Toro, P2×4 receptor in silico and electrophysiological approaches reveal insights of ivermectin and zinc allosteric modulation, *Front Pharm.* 8 (2017), <https://doi.org/10.3389/fphar.2017.00918>.
- [28] J.A. Layhadi, S.J. Fountain, P2×4 receptor-dependent Ca<sup>2+</sup> influx in model human monocytes and macrophages, *Int J. Mol. Sci.* 18 (2017), <https://doi.org/10.3390/ijms18112261>.
- [29] A. Priel, S.D. Silberberg, Mechanism of ivermectin facilitation of human P2×4 receptor channels, *J. Gen. Physiol.* 123 (2004) 281–293, <https://doi.org/10.1085/jgp.200308986>.
- [30] A. Karasawa, T. Kawate, Structural basis for subtype-specific inhibition of the P2×7 receptor, *Elife* 5 (2016), <https://doi.org/10.7554/eLife.22153>.
- [31] R. Andrejew, Á. Oliveira-Giacomelli, D.E. Ribeiro, T. Glaser, V.F. Arnaud-Sampaio, C. Lameu, H. Ulrich, The P2×7 receptor: central hub of brain diseases, *Front Mol. Neurosci.* 13 (2020), <https://doi.org/10.3389/fnmol.2020.00124>.
- [32] R. Lara, E. Adinolfi, C.A. Harwood, M. Philpott, J.A. Barden, F. Di Virgilio, S. McNulty, P2×7 in cancer: from molecular mechanisms to therapeutics, *Front Pharm.* 11 (2020), <https://doi.org/10.3389/fphar.2020.00793>.
- [33] L.E.B. Savio, P. de, A. Mello, C.G. da Silva, R. Coutinho-Silva, The P2×7 receptor in inflammatory diseases: angel or demon? *Front Pharm.* 9 (2018) 52, <https://doi.org/10.3389/fphar.2018.00052>.
- [34] P.A.F. Pacheco, L.P. Dantas, L.G.B. Ferreira, R.X. Faria, Purinergic receptors and neglected tropical diseases: why ignore purinergic signaling in the search for new molecular targets, *J. Bioenerg. Biomembr.* 50 (2018) 307–313, <https://doi.org/10.1007/s10863-018-9761-0>.
- [35] D. de Luna Martins, A.A. Borges, N.A. do A. e Silva, J.V. Faria, L.V.B. Hoelz, H.V.C. M. de Souza, M.L. Bello, N. Boechat, V.F. Ferreira, R.X. Faria, P2×7 receptor inhibition by 2-amino-3-aryl-1,4-naphthoquinones, *Bioorg. Chem.* 104 (2020), <https://doi.org/10.1016/j.bioorg.2020.104278>.
- [36] E. Pisylyagin, S. Kozlovskiy, E. Menchinskaya, E. Chingizova, G. Likhatskaya, T. Gorpenchenko, Y. Sabutskiy, S. Polonik, D. Aminin, Synthetic 1,4-naphthoquinones inhibit P2×7 receptors in murine neuroblastoma cells, *Bioorg. Med Chem.* 31 (2021), <https://doi.org/10.1016/j.bmc.2020.115975>.
- [37] R.X. Faria, F.H. Oliveira, J.P. Salles, A.S. Oliveira, N.L. von Ranke, M.L. Bello, C. R. Rodrigues, H.C. Castro, A.R. Louvis, D.L. Martins, V.F. Ferreira, 1,4-Naphthoquinones potentially inhibiting P2×7 receptor activity, *Eur. J. Med Chem.* 143 (2018) 1361–1372, <https://doi.org/10.1016/j.ejmech.2017.10.033>.
- [38] S. Chen, X. Wu, Z. Yu, Juglone suppresses inflammation and oxidative stress in colitis mice, *Front Immunol.* 12 (2021), <https://doi.org/10.3389/fimmu.2021.674341>.
- [39] M. Mittal, M.R. Siddiqui, K. Tran, S.P. Reddy, A.B. Malik, Reactive oxygen species in inflammation and tissue injury, *Antioxid. Redox Signal* 20 (2014) 1126–1167, <https://doi.org/10.1089/ars.2012.5149>.
- [40] T. Ahmad, Y.J. Suzuki, Juglone in oxidative stress and cell signaling, *Antioxidants* 8 (2019), <https://doi.org/10.3390/antiox8040091>.
- [41] N.H. Kim, H.K. Kim, J.H. Lee, S. Il Jo, H.M. Won, G.S. Lee, H.S. Lee, K.W. Nam, W. J. Kim, M.D. Han, Juglone suppresses LPS-induced inflammatory responses and NLRP3 activation in macrophages, *Molecules* 25 (2020), <https://doi.org/10.3390/molecules25133104>.
- [42] S. Maruo, I. Kuriyama, K. Kuramochi, K. Tsubaki, H. Yoshida, Y. Mizushima, Inhibitory effect of novel 5-O-acyl juglones on mammalian DNA polymerase activity, cancer cell growth and inflammatory response, *Bioorg. Med Chem.* 19 (2011) 5803–5812, <https://doi.org/10.1016/j.bmc.2011.08.023>.
- [43] C. dos, S. Moreira, T.B. Santos, R.H.C.N. Freitas, P.A.F. Pacheco, D.R. da Rocha, Juglone: a versatile natural platform for obtaining new bioactive compounds, *Curr. Top. Med Chem.* 21 (2021) 2018–2045, <https://doi.org/10.2174/1568026621666210804121054>.
- [44] Study of CE-224,535 A Twice Daily Pill To Control Rheumatoid Arthritis In Patients Who Have Not Totally Improved With Methotrexate, (n.d.). (<https://clinicaltrials.gov/ct2/show/NCT00628095>).
- [45] P2×7 Receptor, Inflammation and Neurodegenerative Diseases (NeuroInflam), (n.d.). (<https://clinicaltrials.gov/ct2/show/NCT03918616?term=NCT03918616&draw=1&rank=1>).
- [46] First Time in Human Study Evaluating the Safety, Tolerability, Pharmacokinetics, Pharmacodynamics and the Effect of Food of Single Ascending Doses of GSK1482160, (n.d.). (<https://clinicaltrials.gov/ct2/show/NCT00849134?term=NCT00849134&draw=2&rank=1>).
- [47] Antidepressant Trial With P2×7 Antagonist JNJ-54175446 (ATP), (n.d.). (<https://clinicaltrials.gov/ct2/show/NCT04116606?term=NCT04116606&draw=2&rank=1>).